

# Heat Transfer Enhancement By Using Different Patterns Of The Receiver Circumference Of The Locally Fabricated

*Khalid Abdullah Muhammad\**  , *Yaseen H. Mahmood*  , *Othman K. Zidane*  

Department of Physics, College of Science, University of Tikrit, Salahaddeen, Iraq.

\*Corresponding Author.

Received 09/11/2023, Revised 17/03/2024, Accepted 19/03/2024, Published Online First 20/11/2024



© 2022 The Author(s). Published by College of Science for Women, University of Baghdad.

This is an open-access article distributed under the terms of the [Creative Commons Attribution 4.0 International License](https://creativecommons.org/licenses/by/4.0/), which permits unrestricted use, distribution, and reproduction in any medium, provided the original work is properly cited.

## Abstract

The current study presents an experimental attempt to enhance the thermal performance of a parabolic solar collector, which is a tube made of copper, by using four different types of receiver coatings. The experiments were conducted with a mass flow rate of 1 L/min, utilizing deionized water as the heat transfer fluid, and a single-axis tracking system (north-south orientation). The experimental tests were carried out in Mosul, Iraq, during selected days of the months (May, June, July) in the year 2023, from 9 AM to 4 PM. The results indicated that when air was used as a type of receiver coating, the highest useful thermal energy value reached 557 watts, the lowest 69 watts, with an average of 335 watts. When using black chrome-coated glass with aluminum fiber that is evacuated of air, the highest useful thermal energy value was 1247 watts, the lowest 146 watts, with an average of 335 watts. As black chrome-coated glass with PCM was used, the highest useful thermal energy value was 620 watts, the lowest 69 watts, with an average of 324 watts. Finally, when transparent white glass was used, the highest useful thermal energy value was 759 watts, the lowest 97 watts, with an average of 427 watts. These results demonstrate that the utilization of black chrome-coated glass with evacuated aluminum fiber provides the best thermal performance compared to the other types of receiver coatings investigated in this study.

**Keywords:** black chrome-plated glass, heat transfer, Parabolic trough, solar thermal, useful thermal energy.

## Introduction

The need for energy in all its forms is increasing, and making it inexhaustible is imperative through its enhancement using alternative (renewable) sources. The sun is regarded as the foremost energy source in this realm; it is virtually limitless and constitutes clean energy, posing no environmental hazards. Solar energy mitigates the adverse effects associated with fossil fuels which emit harmful gases into the environment<sup>1</sup>. The sun serves as an immense reservoir of pure energy, and the energy

that emanates from its rays and reaches the Earth is referred to as solar energy<sup>2</sup>. Sunlight can be converted into other forms of energy, either directly or indirectly. For instance, thermal and electrical energy, which can be harnessed by humans in their daily lives, are examples of such conversions<sup>3</sup>. Research and developments in utilizing thermal energy optimally began before 1970 in a few countries. However, the majority of this research has remained in the academic realm<sup>4</sup>. There are

numerous regions and countries regarded as suitable for harnessing solar energy, depending on their climate<sup>5</sup>. Iraq is one of these countries due to the approximate 4000 hours of sunlight it receives annually. This abundance of sunlight has enabled it to utilize solar energy in various applications<sup>6</sup>. Concentrated Solar Power (CSP) is a widely adopted technology for harnessing solar radiation, considered the optimal method for thermal energy production. The efficiency of CSP and heat acquisition by receivers are crucial and primary factors for future consideration when employing CSP in solar energy applications<sup>7</sup>. Recent studies indicate that enhancing the receiver's thermal conductivity and increasing the air insulation (evacuation) around the receiver have a positive impact on the thermal performance of CSP<sup>8</sup>. The operating principle of solar collectors involves directing incident sunlight onto a highly reflective surface, where the reflected rays are concentrated onto a suitable receiver that absorbs this radiation. Consequently, heat is transferred to a specific heat transfer medium. Concentrated solar systems convert solar radiation into high temperatures. Through these elevated temperatures, it becomes possible to generate mechanical and thermal energy, thereby potentially generating electrical energy<sup>9</sup>. The core concept of Parabolic Trough Collectors (PTC) systems is the capture of solar radiation and its conversion directly into usable heat for various applications<sup>10</sup>. The Equivalent Cut Collector takes the form of equivalent cuts to reflect solar radiation. This, parallel to the collector's axis, is reflected around a series of points along a single line known as the focus line. The surface area of the equivalent cut collector is always covered with highly reflective surfaces to maximize the utilization of solar radiation. This radiation is concentrated at a focus line tube that receives the reflected rays. The thermal energy is then transferred through the tube's wall to a heat transfer fluid, which carries the heat for various applications<sup>11</sup>.

### Previous Studies

The researchers Won *et al.* have designed, built, and tested a preliminary test model for a solar thermochemical receiver using a reaction system to establish a technical database for future subsystem

design efforts. The focus is on experimentally validating computer simulations to create a reliable design tool for predicting the thermal-chemical performance of the receiver with a reasonable degree of confidence. Computational results are compared with experimental results obtained from the unit tested at the University of New Mexico. Reasonable agreement was found under a set of test conditions. It was concluded that the current design provides satisfactory conversion performance and operational flexibility for constructing a complete reactor/receiver unit for use in a 10 to 15 kilo watt dish assembly system. However, further development work is needed to address issues related to catalyst pollution and the compatibility of reactor building materials<sup>12</sup>.

The researchers LEI *et al.* have described the evolution of glass-to-metal seals in equivalent piece receivers and introduced a new method utilizing high-frequency induction heating to bond borosilicate glass to the ends of Cover alloy spindles. Pre-oxidation experiments on Cover were conducted to measure the oxidation weight gain curves during heating. Pre-oxidation of Cover and the sealing process were assessed through a series of tests to measure gas tightness, sealing strength, microstructure of the sealing interface, and thermal shock resistance. The results demonstrated that excellent sealing of glass to Cover could be achieved by increasing the Cover oxidation weight gain by approximately 0.3-0.8 mg/cm<sup>2</sup>. Finally, a new solar receiver device was developed using the novel sealing method<sup>13</sup>.

Liu *et al.* have designed a low-cost evacuated glass tube solar steam generator with a simplified Compound Parabolic Concentrator (CPC) in their paper. It can produce steam exceeding 200 degrees Celsius at pressures ranging from 0.10 to 0.55 mega Pascal. The solar steam generator primarily consists of 60 assembly units with a total aperture area of 32 square meters. Each unit comprises a fully evacuated glass tube, a simplified CPC, and a concentrically placed metal ring tube inserted into the fully evacuated glass tube. The high-viscosity mixture made of high-temperature oil and graphite powder is filled in the annular space between the

inner glass tube and the concentric copper tube to enhance heat transfer from the selective absorber layer to the working fluid flowing in the concentric tube. External experimental studies were conducted to evaluate the actual performance of the designed solar steam generator in summer under various operating conditions. The experimental results showed that the maximum steam outlet temperature could exceed 200 degrees Celsius at a pressure of 0.55 mega Pascal. The current solar steam generator can consistently produce saturated steam at temperatures exceeding 150 degrees Celsius over a pressure range of 0.1 to 0.55 mega Pascal, with a collection efficiency exceeding 0.30. This can be used as a resource for industrial steam with significant potential for various applications<sup>14</sup>.

Lopez *et al.* conducted experiments on a solar receiver consisting of 16 tubes with a capacity of 150 kilowatts, using a dense gas-solid particle suspension (approximately 30% solid volume fraction) flowing upward as a Heat Transfer Fluid (HTF). The pilot was tested under various operating parameters, including the solid mass flow rate 660-1760 kg/h, solar input power 60-142 kW, and particle temperature before entering the solar receiver 40-180 degrees Celsius. The thermal efficiency of the receiver was calculated ranging from 50-90 % for all experimental cases. System responses to variations in solar radiation and solid mass flow rate were also reported<sup>15</sup>.

Dong *et al.* conducted an experimental study on forced convective heat transfer of solar salt in an inclined tube. Various experiments were sequentially conducted within the experimental data range for solar salt at Reynolds numbers between 10,000 and 36,000 and Brant numbers between 4.75 and 8.0. Based on the experimental data, the local heat transfer coefficient and the overall heat transfer coefficient were detailed investigated. Additional correlations about the expected heat transfer performance of solar salt were obtained, and finally, a correlation for heat transfer with forced convection of solar salt was obtained using multiple linear regressions within a deviation of  $\pm 10\%$ <sup>16</sup>.

Famiglietti and Lacuna designed a Linear Fresnel solar collector that provides heat in the

medium temperature range at reduced cost. Direct air heating inside the Linear Fresnel collector eliminates the need for liquid heat transfer fluid and the heat exchanger, reducing installation and maintenance costs, as well as waste. In this study, experimental research was conducted on the first small-scale prototype of a solar field with an area of 79.2 square meters. The applied digital model was adjusted and verified for accuracy. Special attention was given to the performance of the turbines, and the limited efficiency of the turbine charger was determined as pioneering research<sup>17</sup>.

Alexandre Bittencourt *et al.* described a set of iterative procedures developed in Matlab and Engineering Equation Solver. These procedures were used to experimentally obtain the optical characterization and heat loss for a small-scale linear Fresnel condenser. These procedures were created for an initial model designed and manufactured to generate direct steam by the LEPTEN laboratory at the Federal University of Santa Catharina. Two different sets of experimental data were considered. Firstly, the heat transfer fluid at the lowest achievable temperature was used with the available experimental setup to obtain peak optical efficiency and incident angle rate. The second set, with a wider range of liquid temperatures, was used to find heat loss. By applying the developed procedures, convergence was achieved. The peak optical efficiency ranged from 47 % to 52 %. Monte Carlo Ray-Tracing software was used to obtain the incident angle rate, and these curves were compared with the experimental curves. A heat loss curve was created for liquid temperatures up to 130 degrees Celsius. These iterative procedures can be adapted to determine heat loss and optical efficiency in any linear Fresnel solar condenser if sufficient experimental data is available. Each program used had its role, and the combined use of both allowed for a rapid and easily converging methodology<sup>18</sup>.

Lee JY *et al.* identified perspectives and expectations for the first and second life of lithium-ion energy storage systems in various applications within the distribution grid system that aligns with current policies in Malaysia. This paper also sheds

light on technical and non-technical reviews of energy storage technologies. The research results indicate that the application of energy storage demonstrates better performance alongside the integration of renewable energy sources compared to current technologies in the Malaysian grid system. Additionally, second-life lithium-ion batteries with 80% remaining capacity can enhance the current economic value of Energy Storage Systems (ESS) over their service life<sup>19</sup>.

Alaskaree studied a solar-powered system for long-term energy and fresh water supplies, combining energy generation and a sub cycle for water production. The system achieves maximum values for the freshwater production rate, water temperature, glass temperature, which are inversely related to the basin water's heat capacity. A single-sided solar distillation device was compared with another equipped with six parallel columns and a horizontal mirror, achieving maximum efficiencies of 49.14% and 18.91%, respectively. The goal is to find the best design to increase clean freshwater production in the shortest time possible and utilize recycled materials in the distillation system<sup>20</sup>.

Wang *et al.* proposed a multi-functional heat pump using the refrigerant R417A, combining a Direct Expansion Solar Heat Pump (DXSHP) and an Air Source Heat Pump (ASHP). This results in a Direct Expansion Solar/Air Source Heat Pump (DX-S/ASHP). The results showed that in the combined cooling and heating mode, the average Coefficient of Performance (COP) can approach 6.0. In the DX-SHP mode, the average COP for domestic hot water heating and space heating is 3.94 and 4.25, respectively, higher than the air

source heat pump under similar working conditions. Switching from DX-SHP to ASHP for domestic hot water heating is necessary only when solar radiation is less than 300 W/m<sup>2</sup>, while the transition to ASHP for space heating is necessary only in the absence of solar radiation. As the working temperature increases, COP decreases, while the working temperature has a minimal effect on the thermal collection efficiency<sup>21</sup>.

### Statement of the Problem

The research problem lies in the effect of the types of receiving tubes on the thermal performance of the solar collector.

### The Proposed Solution for the Problem

To harness solar radiation, solar collectors are employed. The optimal type of collector is the Equivalent Solar Collector. To enhance its performance, various types of surrounding environments were utilized. In this study, four types of surrounding environments were used: First, air. Second, black chrome-coated glass with aluminum fiber (a porous material) and evacuated air. Third, black chrome-coated glass with phase change material. Fourth, transparent white glass evacuated of air.

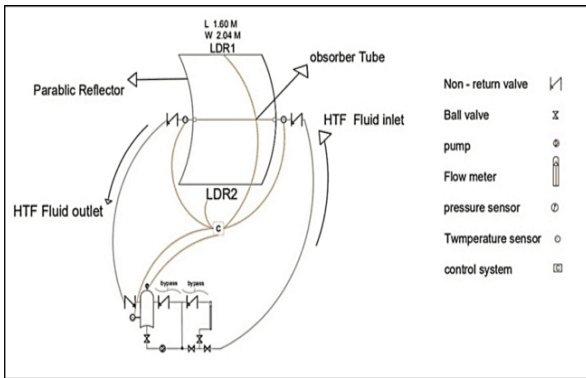
### Objective of the Study

Studying the impact of receiver circumference on the thermal performance of the locally manufactured solar collector system in the city of Mosul - Iraq, which is located at longitude 43.015° and latitude 36.316°. The best in terms of thermal performance and improved heat transfer are chosen.

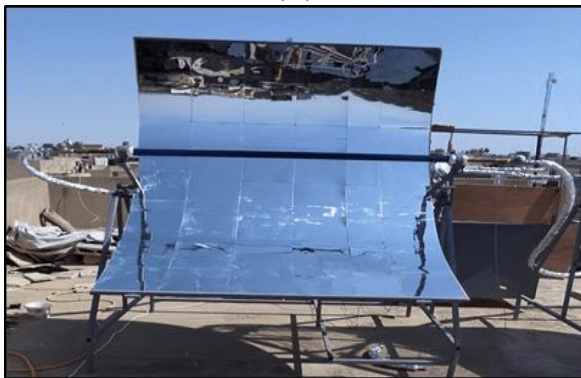
## Materials and Methods

### The PTC Model

The parabolic trough system was designed and constructed using local materials from Mosul, Iraq, as in Fig1:



(A)



(B)



(C)

**Figure 1. (A) General layout of the equivalent trough system, (B) Solar concentrator and (C) Storage and control system.**

### Solar Concentrator System

This system comprises the following components:

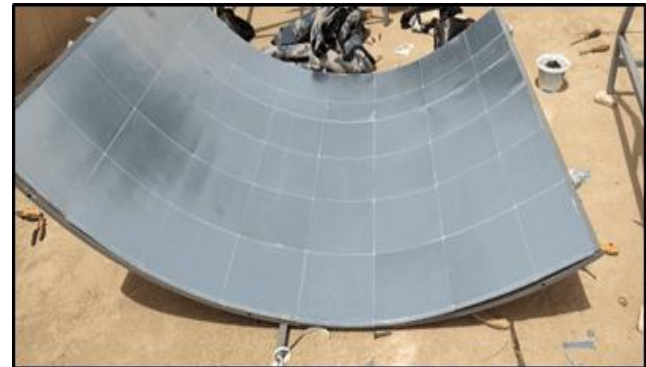
#### Reflective Surface

First, the bendable wooden panels are placed, with a length of 2.30 m, a width of 1.70 m, and a thickness of 7 mm, inside the iron rail (edge) fixed onto the metal frame. Then, a polymer mirror,

measuring 30 cm in length, 30 cm in width, and 1.5 mm in thickness, was affixed. See Fig 2 (A and B).



(A)



(B)

**Figure 2. (A) Placement of wooden panels as an insulating material. (B) Polymer mirror adhesive.**

### The Receiver

Four types of receivers were utilized, namely copper tube no cover (CTNC), copper tube coated with black chrome-coated glass and aluminum fiber (CTBCGAF), copper tube coated with black chrome-coated glass and phase change material (CTCBCGPC) and copper tube coated with transparent white glass (CTCG) described as follows.

#### A- Copper Tube no cover (CTNC)

A copper tube is used with a length of 2 m, an outer diameter of 2.54 cm, an inner diameter of 2.34cm, and a thickness of 0.2 mm. A coupling with a diameter of 22 mm was welded at both ends to connect with the fluid-carrying pipes entering and exiting the tank. An opening is also made and attaching a coupling with a diameter of 10 mm at the end to attach a temperature sensor for measuring

the inflow and outflow fluid temperatures. See Fig (5-A).

### **B- Copper tube coated with black chrome-coated glass and aluminum fiber (CTBCGAF)**

The same procedure described in point A was repeated, but the copper tube was enveloped with a porous material (aluminum fiber) by a thickness of 1.20 cm and a length of 160 cm. Then, the aluminum fiber-coated copper tube was encased in a black chrome-coated borosilicate glass commonly used in solar heaters, after being cut from the ends using a wire jack device with a length of 1.70 m, an outer diameter of 4.7cm, an inner diameter of 4.38

cm, and a thickness of 3.2 mm. Subsequently, an insulating mica washer was placed with an outer diameter of 4.23 cm and an inner diameter of 4.38 cm. A hole with an outer diameter of 5 mm was created to insert a copper tube measuring 12 cm in length for air evacuation between the copper and glass tubes. This copper tube was inserted at the ends between the copper and borosilicate glass tubes, with an internal gap of 5 cm. Following this, the gap was filled with insulating epoxy material, measuring 5 cm in length and 1.84 cm in thickness, to complete the evacuation process using an air evacuation device at a pressure of (-50 cmHg). See Figs 3 and (5-B).



**Figure 3. Primary materials for the copper tube surrounded by aluminum fiber and black chrome-coated glass.**

### **C- Copper tube coated with black chrome-coated glass and phase change material (CTCBGPC)**

The steps outlined in point B were repeated, but instead of using aluminum foam, phase change material was utilized with a length of 160 cm and a thickness of 1.84 cm. See Figs 4 and (5-C).



**Figure 4. Primary materials for the copper tube surrounded by phase change material and black chrome-coated glass.**

#### D- Copper tube coated with transparent white glass (CTCG)

The steps explained in points A and B were repeated, but this time a transparent white glass

commonly used in solar heaters is utilized, with a length of 1.70 meters, an outer diameter of 5.8 cm, an inner diameter of 5.48 cm, and a thickness of 3.2 mm. See Fig (5-D).



**Figure 5. Types of receivers used in the study. (A) Copper tube surrounded by air. (B) Copper tube surrounded by aluminum fiber, black chrome-coated glass, and vacuum. (C) Copper tube surrounded by phase change material and black chrome-coated glass. (D) Copper tube coated by transparent white vacuum-sealed glass.**

#### Tank System and Connecting Pipes

A pressurized tank with a capacity of 13.6 liters is utilized, capable of withstanding pressures up to 50 bar. Openings are created on each side for fluid inlet and outlet. An opening was positioned on the upper right surface for the vapor pressure sensor, and another on the lower right surface for the temperature sensor of the fluid inside the tank. A bottom opening was designed for fluid egress towards the pump, equipped with a safety valve. The tank was insulated on all sides using a 10 cm thick layer of thermal glass wool to ensure efficient heat insulation. Non-return valves were connected to the side openings, along with a ball valve at the bottom opening to control fluid flow towards the pump.

The tank system consists of two lines: the first intended for aqueous fluids and the second for oils. For connecting pipes, we employed thermal plastic pipes for the tank system, and for the external connecting pipes (inlet and outlet) to the receiver, we utilized thermal cloth pipes. All connecting pipes were coated with heat-insulating foam and subsequently wrapped with thermal siphon. This

arrangement guarantees effective thermal insulation. See Fig (1-C).

#### PTC Receiver Thermal Analysis

Three heat transfer processes occur in a PTC receiver after it is covered with a glass tube: conduction, convection, and radiation. Conduction: It is the transfer of heat from one place to another through the movement of the heat-carrying fluid. This transport depends to a large extent on the physical properties of the fluids and the geometry of the system<sup>22</sup>. Convection: occurs between the inner surface of the absorbing tube and the heat transfer medium<sup>23</sup>. Radiation: Occurs between the outer surface of the absorbent tube, the glass envelope and the atmospheric environment and is highly dependent on the wind<sup>24</sup>. Heat transfer can be reflected, absorbed, or transmitted and produces an exchange of thermal energy<sup>25</sup>. Heat transfer can be studied in three parts: between the inner surface of the absorption tube and the heat transfer fluid, between the receiving tube and the glass cover, and between the glass cover and the sky<sup>26</sup>. This is shown in Fig 6.

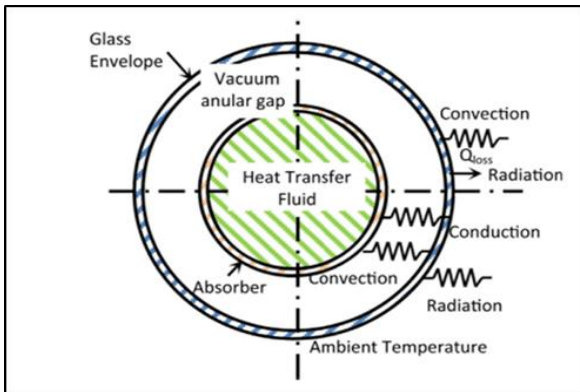


**Figure 6. Cross-sectional scheme of a PTC receiver for the Heat Transfer Mode<sup>27</sup>.**

### The Mathematical Model

It is the energy that is gained directly from the solar radiation falling on the parabolic trough, where the fluid acquires it inside the recipient molecule (the focus), and is calculated from the mathematical relationship<sup>28,29</sup>:

$$Q_{usf,f} = \dot{m}_f C_{p,f} (T_{out,f} - T_{in,f}) \quad 1$$

$Q_{usf,f}$ : The amount of useful energy absorbed by the receiver tube (watts).

$\dot{m}_f$ : The mass flow rate of the fluid ( kg/s).

$C_{p,f}$ : The specific heat of the fluid at constant pressure ( J/kg·K).

$T_{out,f}$ : The outlet temperature of the fluid (K).

$T_{in,f}$ : The inlet temperature of the fluid (K).

### Results and Discussion

This section includes the practical results obtained from the experimental tests conducted over three months in the year 2023 (May, June, July). The tests were conducted from 9:00 AM to 4:00 PM, with readings taken every half an hour, maintaining a constant mass flow rate of the fluid at  $\dot{m}=1$  L/min. The heat transfer fluid (HTF) used was deionized water. An ideal clear weather day was selected for studying the thermal performance of the system.

Fig 7, illustrates the practical results for the temperature difference between the inlet and outlet

### The Practical Thermal Efficiency of the System.

It is the ratio between the useful thermal energy ( $Q_{usf,f}$ ) obtained from the system, which is represented by the energy gained by the fluid, and the solar energy reaching the solar collector ( $Q_{sol,in}$ ). It is calculated using the mathematical relationship<sup>30,31</sup>:

$$\eta_{exp} = \frac{Q_{usf,f}}{Q_{sol,in}} \quad 2$$

$\eta_{exp}$ : Practical thermal efficiency (%)

$Q_{usf,f}$ : The amount of useful energy absorbed by the receiver tube (watts).

$Q_{sol,in}$ : Thermal energy reaching the solar collector ( watts).

The amount of thermal energy entering the system ( $Q_{sol,in}$ ) can be calculated using the mathematical relationship:

$$Q_{sol,in} = I_b \cdot A_a \quad 3$$

$Q_{sol,in}$ : Intensity of direct solar radiation ( W/m<sup>2</sup>).

$A_a$ : Area of the aperture for the parabolic Trough collector (m<sup>2</sup>).

A practical calculation of heat losses can be achieved using the mathematical relationship<sup>28,29</sup>:

$$Q_{loss,exp} = Q_{sol,in} - Q_{usf,f} \quad 4$$

$Q_{loss,exp}$ : Practically lost thermal energy ( watts).

of the heat transfer fluid (HTF), obtained using four different surroundings for the receiver. The results showed that when using a CTNC, the highest temperature difference was 8K, and the lowest was 1K, with an average of 4.81K. When using CTBCGAF, the highest temperature difference was 17.9K, and the lowest was 2.1K, with an average of 9.91K. When using CTCBCGPC, the highest temperature difference was 8.9K, and the lowest was 1K, with an average of 4.66K. When using CTCG, the highest temperature difference was



10.9K, and the lowest was 1.4K, with an average of 6.14K. From these results, it can be observed that the highest temperature difference between the inlet and outlet of the heat transfer fluid was achieved when using CTBCGAF. This is consistent with the study conducted by Raheema<sup>32</sup>.

Fig 8, illustrates the practical results for the incoming heat quantity to the system using the studied receiver surroundings. The results showed that when using CTNC, the highest incoming heat quantity was 3029.95 watts, and the lowest was 1934.016 watts, with an average of 2423.89 watts. When using CTBCGAF, the highest incoming heat quantity was 3029.96 watts, and the lowest was 1901.78 watts, with an average of 2580.83 watts. When using CTCBCGP, the highest incoming heat quantity was 3149.22 watts, and the lowest was 1934.02 watts, with an average of 2505.84 watts. When using CTCG, the highest incoming heat quantity was 2965.49 watts, and the lowest was 1482.75 watts, with an average of 2367.451 watts. From these results, it can be observed that the highest incoming heat quantity to the system was achieved when using CTBCGAF. This was consistent with his study Tagle Salazar *et al*<sup>33</sup>.

Fig 9, illustrates the practical results obtained for the useful thermal energy using the four studied receiver surroundings. The results showed that when CTNC, the highest value obtained for useful thermal energy was 557.46 watts, and the lowest was 69.68 watts, with an average of 335.40 watts. When using CTBCGAF, the highest value was 1247.33 watts, and the lowest was 146.33 watts, with an average of 690.79 watts. When using CTCBCGPC, the highest value was 620.18 watts, and the lowest was 69.68 watts, with an average of 324.72 watts. When using CTCG, the highest value was 759.54 watts, and the lowest was 97.55 watts, with an average of 427.84 watts. These results indicate that using CTBCGAF, as the receiver surroundings is the most effective type in this study. This was consistent with his Barbosa, *et al*<sup>34</sup>.

Fig 10, depicts the practical results obtained for thermal energy losses using four different receiver surroundings. The results revealed that when using CTNC, the highest value for thermal energy losses was 2472.49 watts, and the lowest was 1571.28

watts, with an average of 2087.48 watts. When using CTBCGAF, the highest value was 2093.55 watts, and the lowest was 1755.45 watts, with an average of 1890.04 watts. When using CTCBCGPC, the highest value was 2529.04 watts, and the lowest was 1851.53 watts, with an average of 2181.11 watts. When using CTCG, the highest value was 2255.58 watts, and the lowest was 1385.19 watts, with an average of 1939.59 watts. These results indicate that the least thermal energy losses were observed when using CTBCGAF. This was consistent with his study Guerraiche, *et al*<sup>35</sup>.

Fig 11, illustrates the practical results obtained for operational efficiency using four different receiver surroundings. When using CTNC, the highest value for operational efficiency was 18.40%, and the lowest was 3.60%, with an average of 13.35%. When using CTBCGAF, the highest value for operational efficiency was 41.17%, and the lowest was 7.69%, with an average of 25.56%. When using CTCBCGPC, the highest value for operational efficiency was 19.69%, and the lowest was 3.60%, with an average of 12.26%. When using CTCG, the highest value for operational efficiency was 25.61%, and the lowest was 6.58%, with an average of 17.12%. These results indicate that the highest operational efficiency was achieved when using CTBCGAF. This was consistent with his Barbosa, Madiouli, *et al*<sup>36</sup>.

Fig 12, illustrates the vapor pressure generated inside the tank using four different receiver surroundings. When using CTNC, the highest value for vapor pressure was 4.25 bar, and the lowest was 0.02 bar, with an average of 2.66 bar. When using CTBCGAF, the highest value for vapor pressure was 4.46 bar, and the lowest was 0.031 bar, with an average of 3.26 bar. When using CTCBCGPC, the highest value for vapor pressure was 4.49 bar, and the lowest was 0.021 bar, with an average of 2.93 bar. When using CTCG, the highest value for vapor pressure was 4.38 bar, and the lowest was 0.019 bar, with an average of 2.80 bar. These results indicate that the vapor pressure generated inside the tank was comparable between using CTBCGAF, and using CTCBCGPC. This was consistent with his Chaabane *et al*<sup>37</sup>.

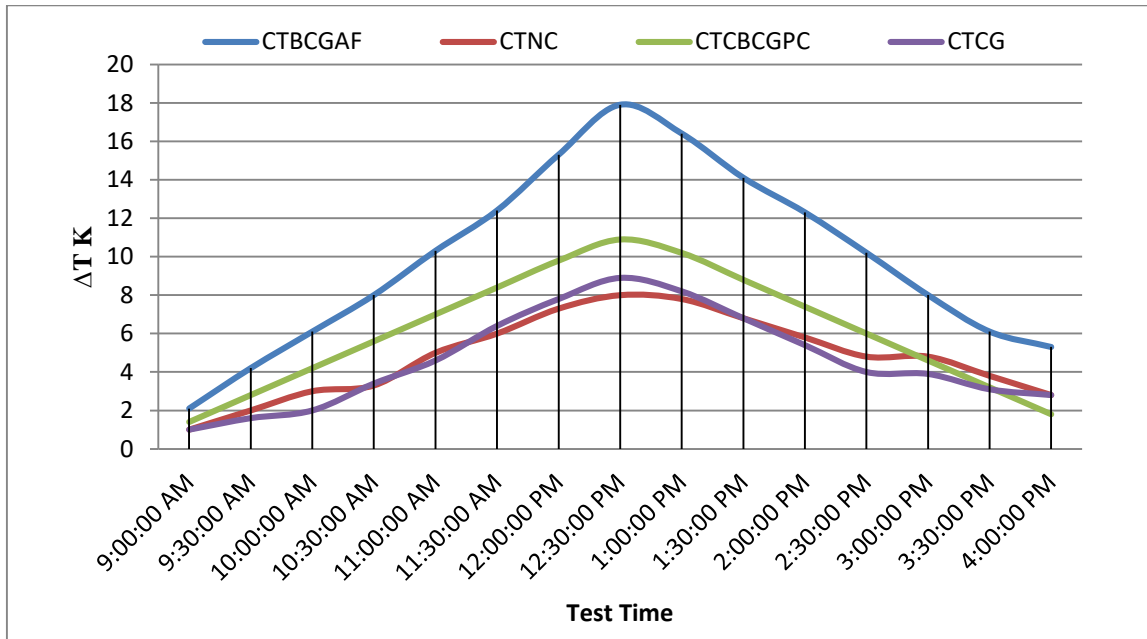


Figure 7. The temperature difference between the inlet and outlet of the fluid using four different receiver surroundings, along with the measurement time.

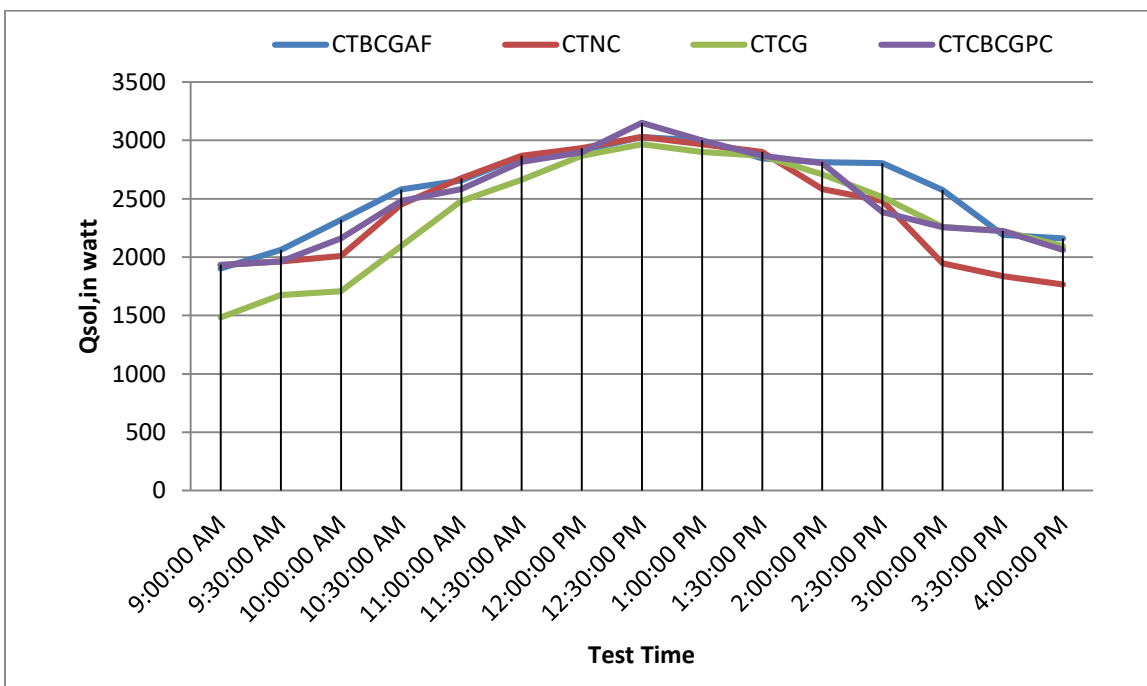
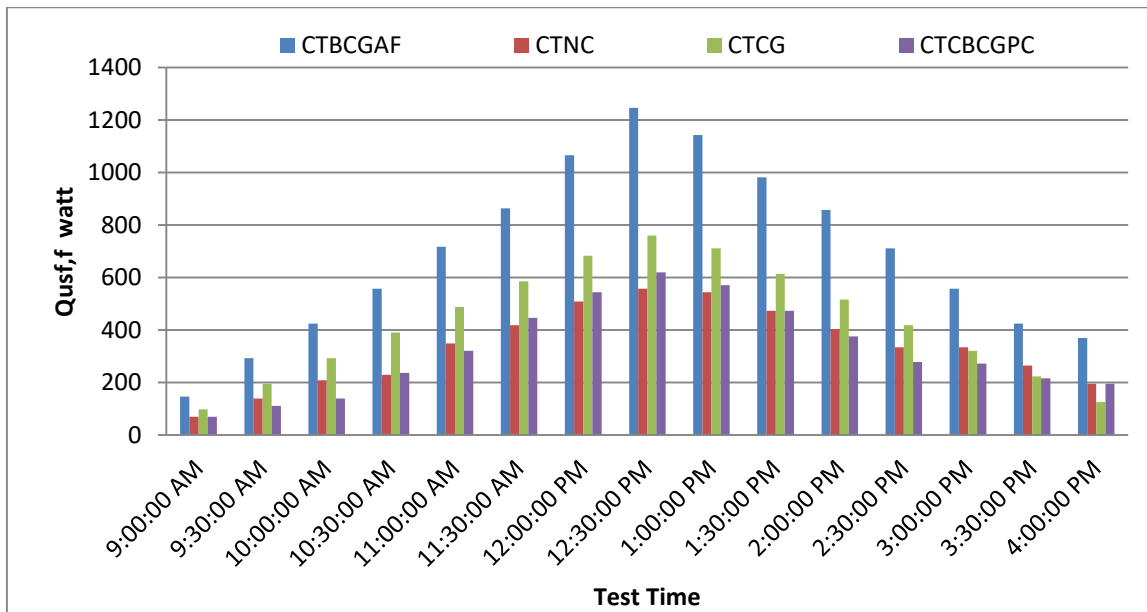
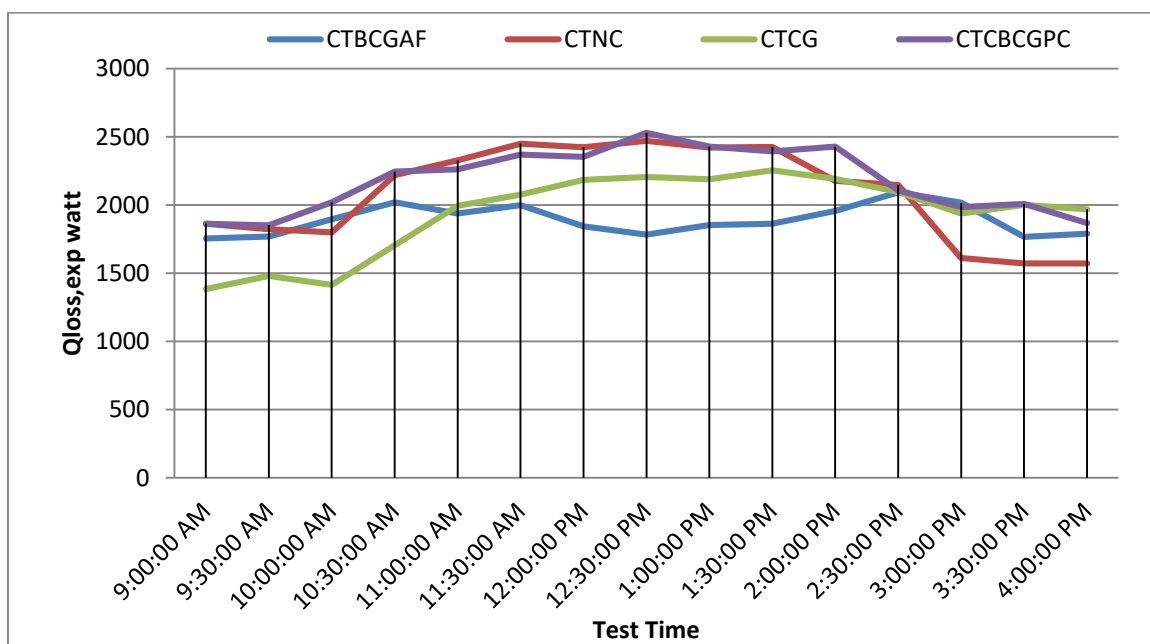


Figure 8. The amount of heat entering the system using four different receiver surroundings, along with the measurement time.



**Figure 9.** The useful heat quantity obtained using four different receiver surroundings, along with the measurement time.



**Figure 10.** The practical heat losses using four different receiver surroundings, along with the measurement time.

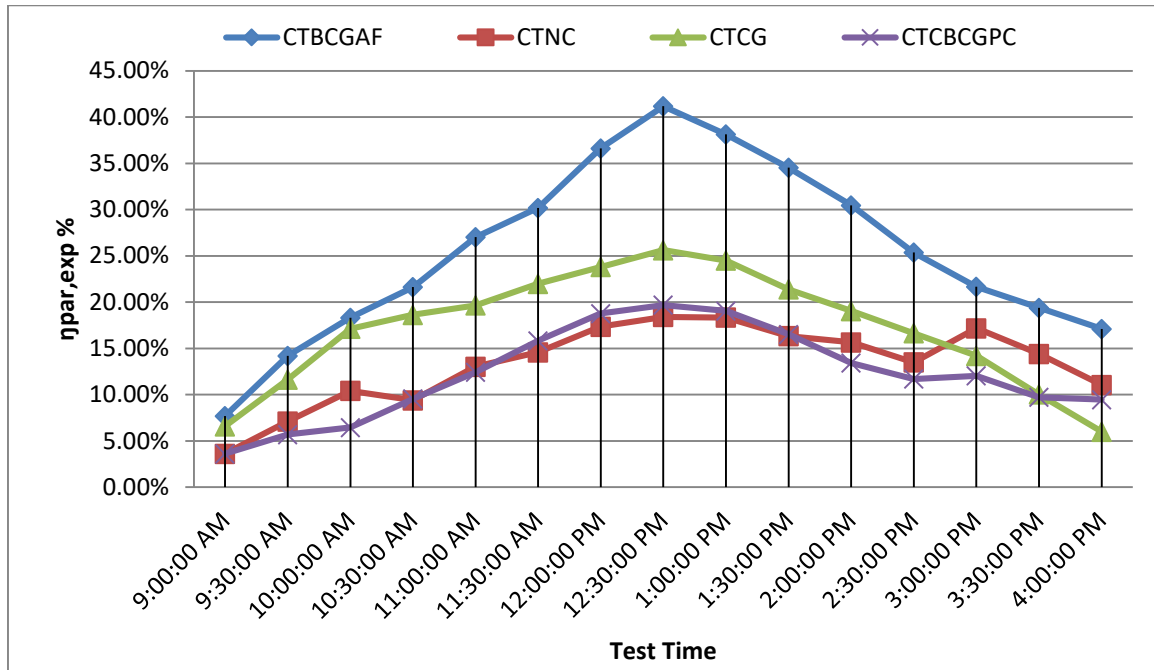


**Figure 11. The practical thermal efficiency using four different receiver surroundings, along with the measurement time.**

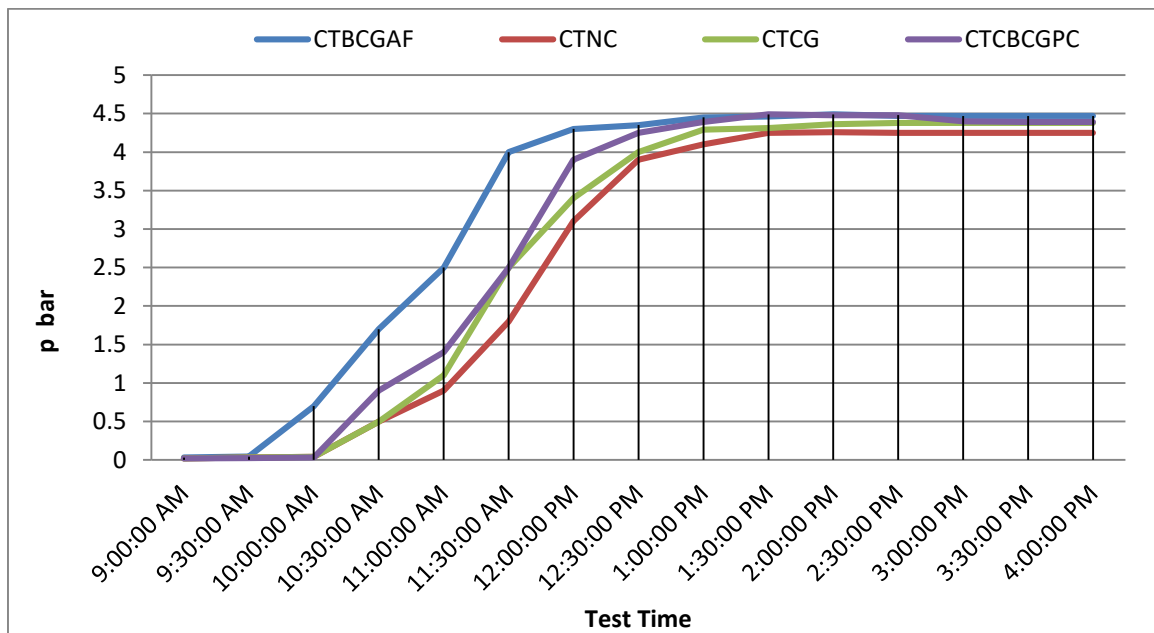


**Figure 12. The generated pressure inside the tank using four different receiver surroundings, along with the measurement time. for the data was averaged.**

### Conclusion

The current study aims to investigate various configurations for the future perimeter of an

equivalent pool-type solar collector and to select the optimal one based on thermal performance. The

pool-type solar collector is locally manufactured using lightweight and cost-effective materials readily available in the local markets of Mosul, Iraq. After obtaining the results, the following conclusions were drawn:

1-The optimal configuration for the collector's perimeter consists of an aluminum fiber (porous material) and a black chrome-coated glass cover, with the space between them evacuated. This configuration exhibited the highest efficiency,

delivered the highest useful heat, and exhibited the lowest heat losses.

2-Evacuating the air between the copper tube (absorber) and the surrounding glass in the collector's perimeter is preferable, as it enhances overall thermal performance.

3-Solar tracking systems are crucial and necessary to enhance the overall thermal efficiency of solar collectors.

## Acknowledgments

We would like to express our deep gratitude and sincere thanks to everyone who contributed to the successful completion of this work. Special thanks go to our esteemed supervisors, as well as the dean of the College of Engineering at the University of Mosul. We also extend our appreciation to the staff

of the Quality Control Laboratory in the College of Engineering, Department of Mechanical Engineering, University of Mosul, for providing their valuable advice, guidance, and valuable insights. Success comes from God's blessings.

## Author's Declaration

- Conflicts of Interest: None.
- We hereby confirm that all the Figures and Tables in the manuscript are ours. Furthermore, any Figures and images, that are not ours, have been included with the necessary permission for re-publication, which is attached to the manuscript.

- No animal studies are present in the manuscript.
- No human studies are present in the manuscript.
- Ethical Clearance: The project was approved by the local ethical committee at University of Tikrit.

## Author's Contribution Statement

Kh. A. M. and O. K. Z. wrote the manuscript, corrected the errors, and conducted the present work by mastering the program used and interpreting the data. Supervisor Y. H. M. set the mechanism of

action in the current study and refined the research by eliminating errors. The authors carefully read the manuscript and approved its final version for this research.

## References

1. Zaboli M, Saedodin S, Mousavi Ajarostaghi SS, Nourbakhsh M. Numerical evaluation of the heat transfer in a shell and corrugated coil tube heat exchanger with three various water-based nanofluids. *Heat Transf.* 2021 Sep; 50(6): 6043-67. <https://doi.org/10.1002/htj.22161>
2. Dawood MM, Nabil T, Kabeel AE, Shehata AI, Abdalla AM, Elnaghi BE. Experimental study of productivity progress for a solar still integrated with parabolic trough collectors with a phase change material in the receiver evacuated tubes and in the still. *J Energy Storage.* 2020 Dec 1; 32: 102007. <https://doi.org/10.1016/j.est.2020.102007>
3. Ebrazeh S, Sheikholeslami M. Applications of nanomaterial for parabolic trough collector. *Powder Technol.* 2020 Sep 20; 375: 472-92. <https://doi.org/10.1016/j.powtec.2020.08.005>
4. Balaji S, Nathani K, Santhakumar R. IoT technology, applications and challenges: a contemporary survey.

- Wirel Pers Commun. 2019 Sep 15; 108: 363-88.  
<https://doi.org/10.1007/s11277-019-06407-w>
5. Pachori H, Choudhary T, Sheorey T. Significance of thermal energy storage material in solar air heaters. Mater. Today: Proc, 2022 Jan, 1( 56). ; 126-134.  
<https://doi.org/10.1016/j.matpr.2021.12.516>
  6. Hakeem HS, Abbas NK. Preparing and studying structural and optical properties of Pb1-xCdxS nanoparticles of solar cells applications. Baghdad Sci J. 2021 Sep 1; 18(3): 0640-648.  
<http://dx.doi.org/10.21123/bsj.2021.18.3.0640> .
  7. Guerraiche D, Bougriou C, Guerraiche K, Valenzuela L, Driss Z. Experimental and numerical study of a solar collector using phase change material as heat storage. J Energy Storage. 2020 Feb 1; 27: 101133.  
<https://doi.org/10.1016/j.est.2019.101133>
  8. Akbarzadeh S, Valipour MS. Energy and exergy analysis of a parabolic trough collector using helically corrugated absorber tube. Renew. Energy. 2020 Aug 1; 155: 735-47.  
<https://doi.org/10.1016/j.renene.2020.03.127>
  9. ALI, Shrooq Jomaa, JALIL, Jalal M, ABD AL-KARIM, Shereen F. Radiation Control of Halogen Lamps Falling on Double Pass Solar Air Heater. IOP Conf. Ser.: Mater. Sci. Eng. (discontin.). 2021; 1094(1): 012021.  
<https://doi.org/article/10.1088/1757-899X/1094/1/012021/meta>
  10. Abass NK, Shanan ZJ, Mohammed TH, Abbas LK. Fabricated of Cu doped ZnO nanoparticles for solar cell application. Baghdad Sci J. 2018 Jun 4; 15(2): 0198-0198.  
<http://dx.doi.org/10.21123/bsj.2018.15.2.0198>.
  11. Gharat PV, Bhalekar SS, Dalvi VH, Panse SV, Deshmukh SP, Joshi JB. Chronological development of innovations in reflector systems of parabolic trough solar collector (PTC)-A review. Renewable Sustainable Energy Rev. 2021 Jul 1; 145(1364-0321): 111002. <https://doi.org/10.1016/j.rser.2021.111002>
  12. Won YS, Voecks GE, McCrary JH. Experimental and theoretical study of a solar thermochemical receiver module. Sol. Energy. 1986 Jan 1; 37(2): 109-118.  
[https://doi.org/10.1016/0038-092X\(86\)90068-X](https://doi.org/10.1016/0038-092X(86)90068-X)
  13. Lei D, Wang Z, Li J, Li J, Wang Z. Experimental study of glass to metal seals for parabolic trough receivers. Renew. Energy. 2012 Dec 1; 48: 85-91.  
<https://doi.org/10.1016/j.renene.2012.04.033>
  14. Liu Z, Tao G, Lu L, Wang Q. A novel all-glass evacuated tubular solar steam generator with simplified CPC. Energy Conv. Manag. 2014 Oct 1; 86: 175-85.  
<https://doi.org/10.1016/j.enconman.2014.04.099>
  15. Lopez IP, Benoit H, Gauthier D, Sans JL, Guillot E, Mazza G, et al. On-sun operation of a 150 kWth pilot solar receiver using dense particle suspension as heat transfer fluid. Sol Energy. 2016 Nov 1; 137: 463-76.  
<https://doi.org/10.1016/j.solener.2016.08.034>
  16. Dong X, Bi Q, Cheng X, Yao F. Convective heat transfer performance of solar salt in an inclined circular tube. App Thermal Eng. 2020 Sep 1; 178: 115349.  
<https://doi.org/10.1016/j.applthermaleng.2020.115349>
  17. Famiglietti A, Lecuona A. Direct solar air heating inside small-scale linear Fresnel collector assisted by a turbocharger: Experimental characterization. App Thermal Eng. 2021 Sep 1; 196: 117323.  
<https://doi.org/10.1016/j.applthermaleng.2021.117323>
  18. de Sá Alexandre Bittencourt, Pigozzo Filho VC, Tadriss L, Passos JC. Experimental study of a linear Fresnel concentrator: A new procedure for optical and heat losses characterization. Energy. 2021 Oct 1; 232: 121019.  
<https://doi.org/10.1016/j.energy.2021.121019>.
  19. Lee JY, Ramasamy AK, Ong KH, Verayiah R, Mokhlis H, Marsadek M. Energy storage systems: a review of its progress and outlook, potential benefits, barriers and solutions within the Malaysian distribution network. J Energy Storage. 2023 Nov 20; 72: 108360. <https://doi.org/10.1016/j.est.2023.108360>
  20. Alaskaree EH. An experimental investigation of the solar distiller basin's performance using a flat mirror and vertical barriers. Case Stud Chem Environ Eng. 2023 Dec 1; 8: 100416.  
<https://doi.org/10.1016/j.cscee.2023.100416>.
  21. Wang C, Gao Y, Dai Z, Wu D, Huang Z, Zhang X, et al. Experimental investigation and performance evaluation on a direct expansion solar-air source heat pump system. Int J Refrig. 2023 Jan 1; 145: 168-76.  
<https://doi.org/10.1016/j.ijrefrig.2022.08.030>
  22. Babikir MH, Njomo D, Barka M, Chara-Dackou VS, Kondji YS, Khayal MY. Thermal modeling of a parabolic trough collector in a quasi-steady state regime. J Renew Sustain Energy. 2021 Jan 1; 13(1).  
<https://doi.org/10.1063/1.5145272>
  23. Kabiri S, Manesh MK, Yazdi M, Amidpour M. Dynamic and economical procedure for solar parallel feedwater heating repowering of steam power plants. App Thermal Eng. 2020 Nov 25; 181: 115970.  
<https://doi.org/10.1016/j.applthermaleng.2020.115970>
  24. Fredriksson J, Eickhoff M, Giese L, Herzog M. A comparison and evaluation of innovative parabolic trough collector concepts for large-scale application. Sol Energy. 2021 Feb 1; 215: 266-310.  
<https://doi.org/10.1016/j.solener.2020.12.017>

25. Shi X, Zhao X, Wang F, Cheng Z, Dong Y, Xu J. Improving overall heat transfer performance of parabolic trough solar receiver by helically convex absorber tube. *App Thermal Eng.* 2022 Aug 1; 213: 118690. <https://doi.org/10.1016/j.applthermaleng.2022.118690>
26. Goyal R, Reddy KS. Numerical investigation of entropy generation in a solar parabolic trough collector using supercritical carbon dioxide as heat transfer fluid. *App Thermal Eng.* 2022 May 25; 208: 118246. <https://doi.org/10.1016/j.applthermaleng.2022.118246>
27. Zhang W, Duan L, Wang J, Ba X, Zhang Z, Tian R. Influences of tracking and installation errors on the optical performance of a parabolic trough collector with heat pipe evacuated tube. *Sustain. Energy Technol Assess.* 2022 Mar 1; 50: 101721. <https://doi.org/10.1016/j.seta.2021.101721>
28. Ahmed M, Shakker, Optimum Design of Parabolic Solar Collector With Exergy Analysis, *Tikrit J Eng Sci.* 2017; 24 (4): 49-57. <https://tj-es.com/wp-content/uploads/2018/10/vol24no4p10.pdf>
29. Mahammed SS, Yassen TA, Khalaf HJ. Theoretical study of the compound parabolic trough solar collector. *Tikrit J Eng Sci.* 2012 Jun 30; 19(2): 1-9. <https://www.iasj.net/iasj/download/28414dbda5d76cc>
30. Raheema YS, Bedaiwi BO. Experimental study of steam generation by parabolic trough concentrator with two axes tracking. *J Eng Sustain* 2021 Jun;15-24. <https://doi.org/10.31272/jeasd.conf.2.2.3>
31. Achkari O, El Fadar A, Amlal I, Haddi A, Hamidoun M, Hamdoune S. A new sun-tracking approach for energy saving. *Renew Energy.* 2021 May 1; 169: 820-35. <https://doi.org/10.1016/j.renene.2020.12.039>
32. Raheema YS, Bedaiwi BO. Experimental study of steam generation by parabolic trough concentrator with two axes tracking. *J Eng Sustain Dev (JEASD).* 2021 Jun; (2520-0925: (Conference proceedings 2021). <https://www.iasj.net/iasj/download/97c6220bc3f1864b>
33. Tagle-Salazar PD, Nigam KD, Rivera-Solorio CI. Parabolic trough solar collectors: A general overview of technology, industrial applications, energy market, modeling, and standards. *Green Process. Synth.* 2020 Nov 23; 9(1): 595-649. <https://doi.org/10.1515/gps-2020-0059>
34. Barbosa EG, Martins MA, de Araujo ME, dos Santos Renato N, Zolnier S, Pereira EG, et al. Experimental evaluation of a stationary parabolic trough solar collector: Influence of the concentrator and heat transfer fluid. *J Clean Prod.* 2020 Dec 10;276:124174. <https://doi.org/10.1016/j.jclepro.2020.124174>
35. Guerraiiche D, Bougriou C, Guerraiiche K, Valenzuela L, Driss Z. Experimental and numerical study of a solar collector using phase change material as heat storage. *J Energy Storage.* 2020 Feb 1; 27: 101133. <https://doi.org/10.1016/j.est.2019.101133>
36. Madiouli J, Saleel CA, Lashin A, Badruddin IA, Kessentini A. An experimental analysis of single slope solar still integrated with parabolic trough collector and packed layer of glass balls. *J Therm Anal Calorim.* 2021 Dec; 146: 2655-65. <https://link.springer.com/article/10.1007/s10973-020-10320-x>
37. Chaabane M, Mhiri H, Bournot P. Thermal performance evaluation and enhancement of a parabolic trough collector. *J. Renew. Sustain Energy.* 2020 Jul 1; 12(4): 20-33. <https://doi.org/10.1063/1.5145257>

## تحسين انتقال الحرارة باستخدام أنماط مختلفة من محيط المستقبل المصنع محليا

خالد عبدالله محمد علي، ياسين حميد محمود ، عثمان خلف زيدان

قسم الفيزياء، كلية العلوم، جامعة تكريت، صلاح الدين، العراق.

### الخلاصة

العمل الحالي تمت محاولة تجريبية لتحسين الاداء الحراري للجامع الشمسي نوع حوض مكافئ باستخدام اربعة انواع مختلفة من المحيط بالمستقبل. عند سرعة تدفق كتلي 1L/min، استخدمنا ماء منزوع الايونات كمائع ناقل للحرارة ونظام تتبع احادي المحور (شمال-جنوب). الاختبار التجريبي تم في مدينة الموصل-العراق خلال ايام مختارة من الاشهر (أيار، حزيران، تموز) سنة 2023 خلال وقت النهار (9 صباحاً – 4 مساءً). بينت النتائج عندما يكون الهواء هو محيط بالمستقبل كانت الطاقة الحرارية المفيدة اعلى قيمة لها تساوي 557watt و اقل قيمة 69watt وبمعدل 335watt. عند استخدام الزجاج المطلي بالكروم الاسود مع ليف المنيوم ويكون مفرغ من الهواء كانت الطاقة الحرارية المفيدة اعلى قيمة لها تساوي 1247watt و اقل قيمة 146watt وبمعدل 335watt. عند استخدام الزجاج المطلي بالكروم الاسود مع مادة القير كانت الطاقة الحرارية المفيدة اعلى قيمة لها تساوي 620watt و اقل قيمة 69watt وبمعدل 324watt. عند استخدام زجاج ابيض شفاف كانت الطاقة الحرارية المفيدة اعلى قيمة لها تساوي 759watt و اقل قيمة 97watt وبمعدل 427watt. هذه النتائج تبين، استخدام الزجاج المطلي بالكروم الاسود مع ليف المنيوم ويكون مفرغ من الهواء يعطي افضل اداء حراري بالمقارنة مع الانواع الاخرى من المحيط بالمستقبل المستخدمة في هذا العمل.

**الكلمات المفتاحية:** زجاج مطلي بالكروم الأسود، نقل الحرارة، حوض مكافئ، الطاقة الشمسية الحرارية، طاقة حرارية مفيدة.